

this case will be possible. In this case ($\beta \ll 1$) one obtains a frequency splitting

$$\Delta\omega/\omega = (9/2)v_T^2/c^2 = 8.8 \times 10^{-3} T_e(\text{keV})$$

corresponding to the fastest-growing mode $\mathbf{k} \approx \mathbf{k}_0$ in Eq. (2).

We have extended our calculations to the case of oblique incidence of the pump, and reached two important conclusions.⁹ First, the threshold for two-plasmon decay is reduced by a factor of approximately $\cos\theta$, θ being the angle between the pump wave vector and the density gradient in the unstable region. This is the case for both s- and p-polarization. Second, in the case of p-polarization the growth rate is no longer a symmetric function of k_\perp : plasma waves with wave vectors more oblique to the gradient are found to be more unstable.

In summary, it has been found that for typical experimental parameters the expected decay-wave spectrum of the $2\omega_p$ instability depends on the laser wavelength. For long-wavelength (e.g., 10- μm) lasers, plasma waves with large wave vector are most unstable, while for shorter-wavelength ($\leq 1\mu\text{m}$) lasers the opposite is the case. In addition, when the laser is obliquely incident, lower thresholds are expected, and in the case of p-polarization asymmetric plasma-wave spectra are produced.

REFERENCES

1. Y. C. Lee and P. W. Kaw, *Phys. Rev. Lett.* **32**, 135 (1974).
2. C. S. Liu and M. N. Rosenbluth, *Phys. Fluids* **19**, 967 (1976).
3. B. F. Lasinski and A. B. Langdon, Lawrence Livermore 1977 Annual Report UCRL-50021-77.
4. LLE Review **13**, Section 2.D (1982).
5. E. A. Jackson, *Phys. Rev.* **153**, 235 (1967).
6. A. Simon, R. W. Short, E. A. Williams, and T. Dewandre, submitted to *Phys. Fluids*.
7. H. A. Baldis and C. J. Walsh, *Phys. Fluids* **26**, 1364 (1983).
8. D. M. Villeneuve, R. L. Keck, B. B. Afeyan, W. Seka, and E. A. Williams (to be published).
9. B. B. Afeyan, E. A. Williams, R. W. Short, and A. Simon, *Bull. Am. Phys. Soc.* **27**, 951 (1982).

2.C Broadband Spectrally Resolving X-Ray Instrumentation

The examination of the spectral characteristics of x-ray emission from high-density plasmas has long been utilized as an effective diagnostic of the plasma state. The diagnosis of laser-produced plasmas makes special requirements of x-ray spectroscopic techniques in that extremes of temperature and density are created within microscopic regions and evolve in time on an ultrafast

timescale. There is currently a strong interest in such plasmas, notably because of their utilization in various laser-fusion and x-ray-laser schemes, but also because of a more general need to understand the rich variety of interaction mechanisms possible in such plasmas. In addition, laser-produced plasmas show considerable potential as ultrashort, high-fluence x-ray sources, suitable for a wide variety of applications such as x-ray flash radiography, kinetic x-ray diffraction, and x-ray absorption spectroscopy.

In general, such studies would be better served by experimental diagnostic techniques which, in addition to spectral resolution, provide spatial discrimination of the origin of the x-ray emission and the capacity to delineate in time its spectral and spatial features. These requirements are nowhere more necessary than in the study of laser-fusion plasmas, where spectrally resolved data in the 0.1–50-keV range is required along with micron spatial accuracy and picosecond temporal resolution.¹

We describe here in detail two x-ray instruments incorporating free-standing x-ray transmission gratings to provide broadband spectral resolution. The first, a spectrally dispersive microscope, may be used to obtain two-dimensional monochromatic spatial images of laser-fusion targets. This instrument has been used to measure the spatial extent of the core of an imploded glass microballoon containing a mixture of deuterium and argon, as reported in an earlier issue of the LLE Review.² The second instrument, a transmission-grating streak spectrograph, allows for the simultaneous temporal and spectral resolution of target x-ray emission.

Spectrally Dispersive Microscope

Line-specific dispersed images can be produced with the incorporation of a low-dispersive-power element into the optical path of an x-ray microscope.³ The most suitable element for this purpose is a free-standing x-ray transmission grating, which introduces negligible optical distortion, is inherently efficient, and is relatively easy to implement. Finely spaced metallic gratings having a spatial period of 300 nm (bar width 180 nm) have recently been developed with grating thicknesses of ~ 600 nm over large areal extents (~ 1 cm²).⁴ In collaboration with N. M. Ceglio of Lawrence Livermore National Laboratory, A. M. Hawryluk of MIT, and C. H. Hooper of the University of Florida, we have integrated such a grating into the optical path of a four-channel Kirkpatrick-Baez microscope. This instrument, shown in Fig. 7, utilizes an array of four cylindrical mirrors with radii of curvature 32.4 m, in a fixed-focus optically contacted array for greater stability. It has a total solid-angle acceptance of $\sim 10^{-6}$ sr, producing a 5 \times magnified image 127 cm from the target with a spatial resolution of ~ 4 μ m. The mirrors are Ni-coated, which in combination with Be and Al K-edge filters gives a spectral acceptance range of 1.5–4.5 keV under the assumption of a Boltzmann x-ray source function of temperature ~ 1 keV. The grating is deployed at a point along the viewing axes of the microscope, 20.3 cm from the mirror

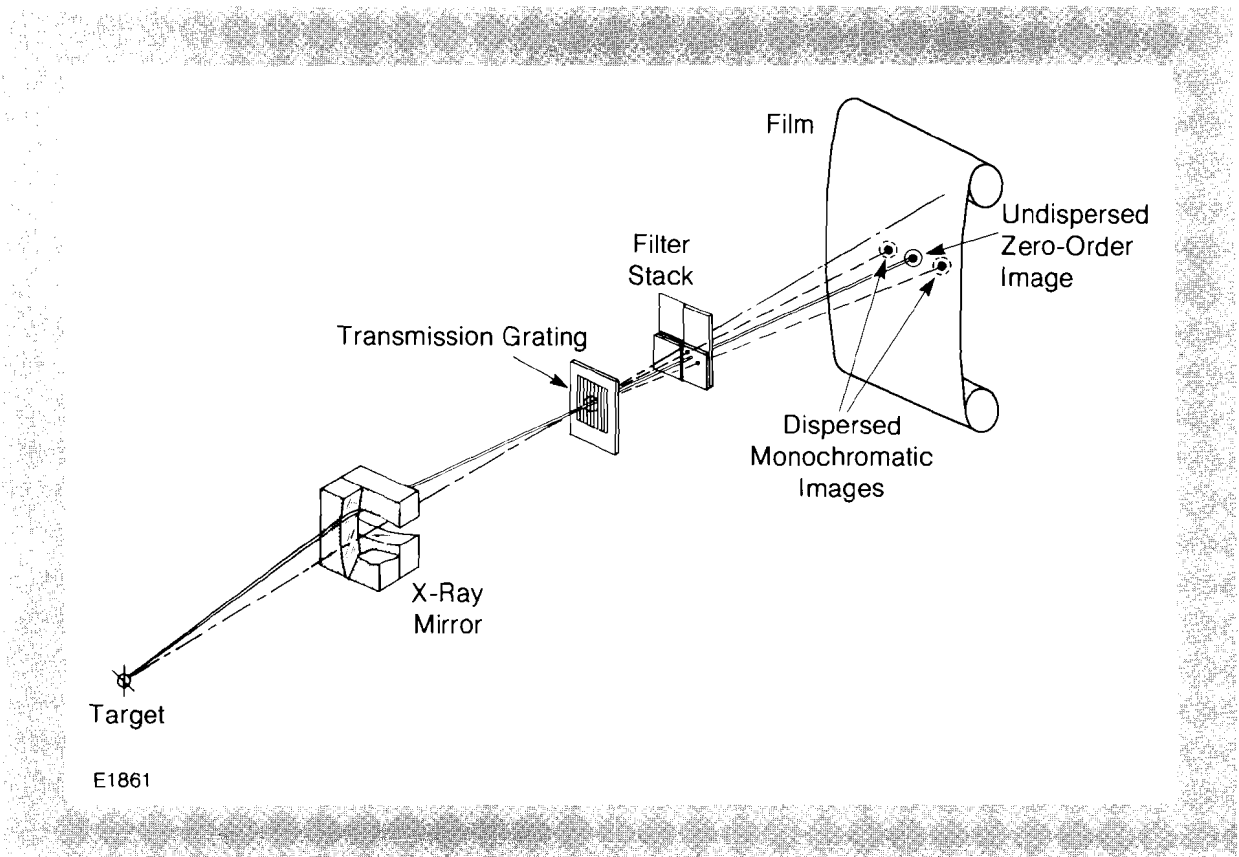


Fig. 7
Schematic of modified Kirkpatrick-Baez microscope. Four images of the target are formed on the film by crossed cylindrical grazing-incidence mirrors. Each image is dispersed spectrally in one direction by the transmission grating and may be selectively filtered in a filter stack.

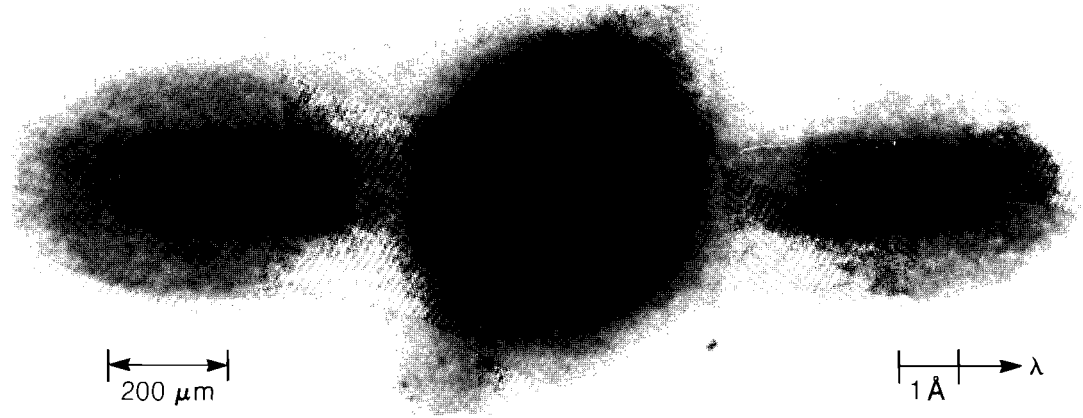
block, where the four microscope image axes intersect. With a distance of 78.7 cm to the image plane, this gives a dispersion of $d\lambda/ds \approx 3.75 \text{ \AA}/\text{mm}$, with an effective spectral resolution in the dispersion direction of $\sim 5 \text{ \AA}$. The spatial resolution in the dispersion-free direction should not be significantly degraded by the imposition of the grating in the optical path.

A typical image from this instrument is reproduced in Fig. 8, showing a multiply dispersed image of a $540\text{-}\mu\text{m}$ -diameter, $1.0\text{-}\mu\text{m}$ -thick glass microballoon imploded by a 1-ns, 2-kJ pulse from the $1.05\text{-}\mu\text{m}$, 24-beam OMEGA laser facility. The central, deliberately overexposed image is one of the four undiffracted (zeroth-order) images produced by the microscope. On either side of this image can be seen the first-order dispersed images of the imploded target. Clear images of the core and corona in emission from He-like and H-like Si and Ca can be determined in the $\sim 6\text{-}\text{\AA}$ range. High-resolution spectrally specific imaging of this type has already proved valuable to the analysis of imploded target cores,² and is expected to be of considerable importance for studies of the stability of imploding shells and for the analysis of two-dimensional features of energy transport and ablation.

Transmission-Grating Streak Spectrograph

Transmission diffraction gratings of the type described above may be deployed in ideal, low-dispersion, broadband spectrographs of high efficiency. In conjunction with an x-ray streak

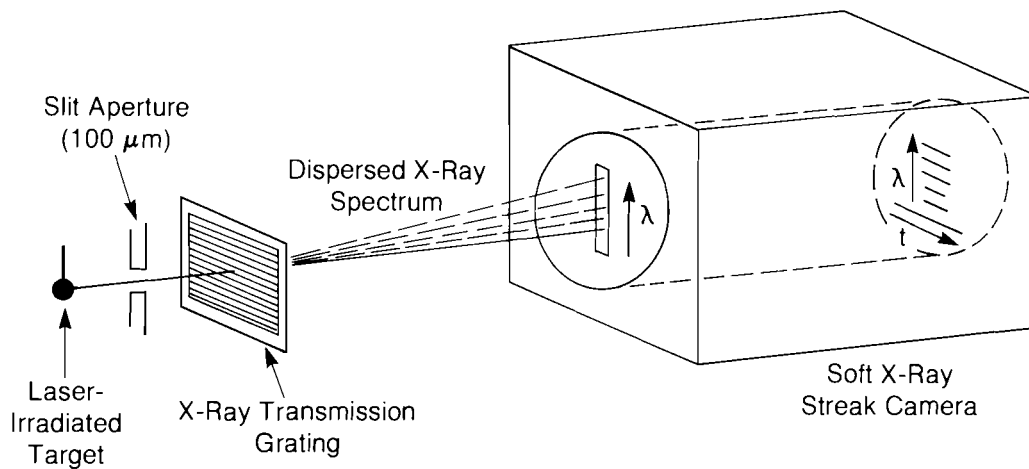
camera, a high-time-resolution spectrograph is created.⁵ In the device constructed at LLE, shown schematically in Fig. 9, a transmission diffraction grating similar to the one described above is mounted together with a 150- μm slit aperture in the path between the target and the streak camera. The x-ray emission from the laser-irradiated target is dispersed along the admittance



E2160

Fig. 8

Dispersed image of a 540- μm -diameter glass microballoon of wall thickness 1 μm , imploded by the OMEGA laser system. The undiffracted (zeroth-order) x rays form a conventional image, overexposed here; first order images are formed from different spectral components diffracted from the zeroth-order image by the transmission grating.



E1863

Fig. 9

Transmission-grating x-ray streak spectrograph. X rays from the target pass through a slit aperture and transmission grating and are dispersed spectrally along the photocathode of the streak camera, which subsequently disperses the spectrum in time. The film record produced represents x-ray intensity as a function of wavelength and time.

slit of the streak camera, which subsequently disperses the spectrum in time.

The streak camera employs a photocathode which consists of 10 nm of gold evaporated onto a 1.5- μm -thick stretched polypropylene substrate. The polyimide substrate of the transmission grating blocks most x rays less energetic than 500 eV. The efficiency of the grating in diffracting x rays more energetic than 500 eV is about 0.1. X rays that pass undiffracted form the zeroth order, from which position the distance of dispersion along the photocathode is proportional to wavelength. The ability of the device to resolve higher-energy x rays, only slightly dispersed in the first order, from the zeroth-order diffraction imposes an upper energy of ~ 10 keV on the dispersed spectrum.

The spectral resolution and dispersion can easily be determined. The grating and slit are placed together, at a distance $L = 108$ cm from the target and at a distance $D = 110$ cm from the streak-camera photocathode. The slit width A is $150 \mu\text{m}$, and the grid is $d = 0.3 \mu\text{m}$. Thus, the spectral resolution in m 'th order ($\delta\lambda$), defined by the equation

$$\delta\lambda = \left[\frac{(S+A)}{L} + \frac{A}{D} \right] \frac{d}{m}$$

is $\approx 1.9 \text{ \AA}$, for a target of source size $S = 400 \mu\text{m}$ as is characteristic of the initial diameter of the spherical targets used in our experiments. The resolution is explicitly dependent on the extent of the emitting region; for sources smaller than about twice the slit-aperture size, the resolution approaches a limiting value of $\sim 0.8 \text{ \AA}$. The spectral dispersion in the streak-camera plane, derived from the Bragg condition $\sin \theta = m\lambda/d$, is $d\lambda/ds = d/mD \approx 2.76 \text{ \AA/mm}$. Thus the 1-cm-long photocathode includes all of the spectrum above the carbon K-edge passed by the polyimide substrate of the transmission grating. The temporal resolution of the streak camera is estimated to be ~ 30 ps.

The large spectral range and good temporal resolution of this device, afforded by the high efficiency of the grating, compensate for the relatively low spectral resolution, and make the device particularly suitable for qualitative and comparative studies. This is illustrated in Fig. 10, which shows the time-resolved spectrum of the x rays emitted from a glass microballoon, of 594- μm diameter and 1.3- μm wall thickness, filled with 20 atm of DT. This was uniformly irradiated with a 1-ns pulse from the 24-beam OMEGA laser system, with a total energy of 2.8 kJ. The brightest time-smearred signal in Fig. 10 is that of the zeroth-order undispersed x-ray emission. However, emission in the first order at $\sim 6 \text{ \AA}$, corresponding predominantly to resonance-line emission from Si in the glass shell, can be seen to persist throughout the irradiation of the target. At the stagnation of the implosion, the core temperature increases, giving rise to a brief, bright emission from the other line radiation, and x-ray continuum in the 1- to 20- \AA range.

Summary

Two new diagnostics have been developed, illustrating the potential of spectrally discriminating space-resolved and time-resolved x-ray instrumentation to the diagnosis of laser-fusion target implosions. These and similar devices will prove valuable to the diagnosis of thermal transport in planar and spherical targets, and to the analysis of the final conditions within imploding spherical targets.

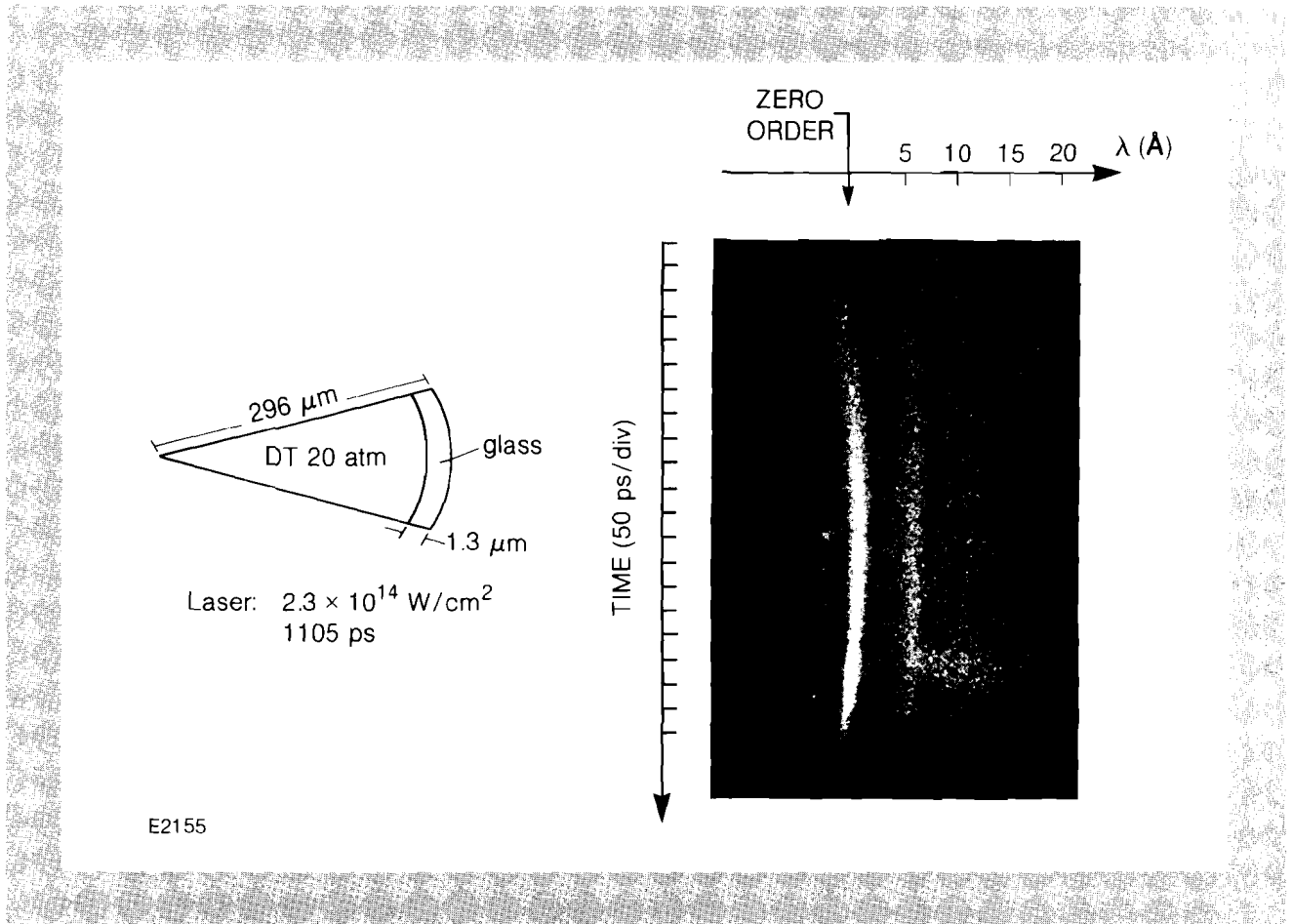


Fig. 10
X-ray streak spectrograph record of a bare glass microballoon imploded by the OMEGA laser system. The undiffracted (zeroth-order) component lasts throughout the laser pulse. The prominent emission at about 6 \AA is Si emission from target shell material; at relatively late times, a broad spectral feature marks the peak implosion of the target.

REFERENCES

1. D. T. Attwood, *IEEE J. Quantum Electron.* **QE-14**, 909 (1978).
2. *LLE Review* **12**, 12 (1982).
3. P. Kirkpatrick and A. V. Baez, *J. Opt. Soc. Am.* **38**, 766 (1948).
4. A. M. Hawryluk, N. M. Ceglio, R. H. Price, J. Melngailis, and H. I. Smith, *Proc. Topical Conf. Low Energy X-Ray Diagnostics*, AIP Conf. Proc. No. 75, p. 286 (1981).
5. N. M. Ceglio, R. L. Kauffman, A. M. Hawryluk, and H. Medici, LLNL Report UCRL-81800 (unpublished) (1982).